# Energies and Derivative Couplings in the Vicinity of a Conical Intersection Using Degenerate Perturbation Theory and Analytic Gradient Techniques. 1

**David R. Yarkony**[†]

*Department of Chemistry, The Johns Hopkins University, Baltimore, Maryland 21218*

*Received: January 8, 1997*[⊗]

Analytic gradient techniques in conjunction with degenerate perturbation theory are used to analyze the energetics and the derivative couplings in the vicinity of a conical intersection. The precision of the analytic gradient based evaluation of the derivative couplings in the vicinity of a conical intersection is established. An approach for the rigorous treatment of two-dimensional Jahn-Teller problems in the absence of $C_{3v}$ symmetry is suggested.

## I. Introduction

Nonadiabatic effects are particularly important in the vicinity of a conical intersection. A complete description of the electronic structure in this region requires both the energies, $E_I(\mathbf{R})$, and derivative couplings, $f_\alpha^{IJ}(\mathbf{R}) = \langle\Psi_I(\mathbf{r};\mathbf{R})|(\partial/\partial R_\alpha)\Psi_J(\mathbf{r};\mathbf{R})\rangle_\mathbf{r}$, where

$$[H(\mathbf{r};\mathbf{R}) - E_I(\mathbf{R})]\Psi_I(\mathbf{r};\mathbf{R}) = 0 \tag{1}$$

and $H(\mathbf{r};\mathbf{R})$ is the nonrelativistic electronic Hamiltonian. In this work the energetics and derivative couplings in the vicinity of a conical intersection are analyzed using degenerate perturbation theory and quantities readily obtained from electronic structure calculations employing analytic gradient techniques. As discussed by Mead[1] and subsequently by Kupperman[2] when the total energy available to a system exceeds the maximum energy on the lower adiabatic potential energy surface along a closed loop surrounding a conical intersection (this energy may be much less than the energy at the conical intersection itself), *adiabatic* nuclear dynamics on that potential energy surface may be altered by the geometric phase effect.[3−7] An approach for analyzing these energetics is suggested. Another goal of this study is to assess the precision of derivative couplings, evaluated with techniques previously introduced by the author together with Lengsfield and Saxe,[8−10] in the vicinity of a conical intersection. This analysis is important since surfaces of derivative couplings determined by *ab initio* techniques for systems exhibiting conical intersections are highly desirable.

Section II presents the theoretical development providing the perturbation analysis and its connection to electronic structure calculations. The perturbation analysis is based on the seminal work of Mead on conical intersections in $X_3$ molecules.[11] See also ref 4. Section III considers the $1^1A' - 2^1A'$ seam of conical intersections in $HeH_2$. This system was selected for analysis because the seam of conical intersections involves nuclear configurations with only $C_s$ symmetry so that symmetry arguments cannot be used to simplify the analysis. This seam of conical intersections is relevant to the electronic quenching reaction

$$H_2(B^1\Sigma_u^+) + He \rightarrow H_2(X^1\Sigma_g^+) + He \tag{2}$$

which has been the subject of much theoretical[12−16] and experimental[17−19] interest in the recent past. Section IV summarizes and suggests directions for future research.

[†] Supported by NSF grant CHE 94-04193.
[⊗] Abstract published in *Advance ACS Abstracts,* May 1, 1997.

## II. Theoretical Approach

The electronic structure calculations employ multiconfigurational self-consistent field (MCSCF)[10]/configuration interaction (CI)[20] wave functions. In the MCSCF/CI approach the adiabatic electronic states, $\Psi_I(\mathbf{r};\mathbf{R})$, are expanded in a configuration state function (CSF)[20] basis

$$\Psi_I(\mathbf{r};\mathbf{R}) = \sum_{\alpha=1}^{N^{\mathrm{CSF}}} c_\alpha^I(\mathbf{R})\,\psi_\alpha(\mathbf{r};\mathbf{R}) \tag{3}$$

where the $\mathbf{c}^I(\mathbf{R})$ satisfy

$$[\boldsymbol{H}(\mathbf{R}) - E_I(\mathbf{R})]\mathbf{c}^I(\mathbf{R}) = \mathbf{0} \tag{4}$$

The molecular orbitals used to build the $\boldsymbol{\psi}(\mathbf{r};\mathbf{R})$ are obtained from a state-averaged MCSCF procedure.[10]

**A. Degenerate Perturbation Theory in a Crude Adiabatic Basis.** Assume that $\mathbf{R}_x$ is a point of intersection of two potential energy surfaces, $E_I(\mathbf{R})$, $I = 1 - 2$. A new basis for $H(\mathbf{r};\mathbf{R})$ is constructed from a fixed, geometry-independent transformation of the CSF basis. The first two components of the basis are $\mathbf{c}^I(\mathbf{R}_x)^\dagger\,\boldsymbol{\psi}(\mathbf{r};\mathbf{R})$, $I = 1 - 2$, satisfying eq 4. Denote this as the *Q*-space. Its orthogonal complement is the *P*-space. The orthonormal functions in the *P*-space, denoted $\mathbf{C}^K(\mathbf{R}_x)^\dagger\,\boldsymbol{\psi}(\mathbf{r};\mathbf{R})$, $K = 3 - N^{\mathrm{CSF}}$, need only be orthogonal to $\mathbf{c}^I(\mathbf{R}_x)^\dagger\,\boldsymbol{\psi}(\mathbf{r};\mathbf{R})$, $I = 1 - 2$. The $\mathbf{C}^K(\mathbf{R}_x)$ are not, in general, eigenfunctions of $\boldsymbol{H}(\mathbf{R}_x)$. This basis has only a limited geometry dependence through the CSFs. It is similar to the "crude adiabatic" basis introduced by Longuet-Higgins in his classic treatment of the Jahn-Teller and Renner-Teller effects[3] and will be denoted as such subsequently.

In the crude adiabatic basis, at any $\mathbf{R}$, eq 4 becomes

$$\begin{pmatrix} \boldsymbol{H}^{QQ}(\mathbf{R}) - \boldsymbol{I}E_I(\mathbf{R}) & \boldsymbol{H}^{QP}(\mathbf{R}) \\ \boldsymbol{H}^{PQ}(\mathbf{R}) & \boldsymbol{H}^{PP}(\mathbf{R}) - \boldsymbol{I}E_I(\mathbf{R}) \end{pmatrix} \begin{pmatrix} \xi^I(\mathbf{R}) \\ \Xi^I(\mathbf{R}) \end{pmatrix} = \begin{pmatrix} 0 \\ 0 \end{pmatrix} \tag{5}$$

where

$$H_{IJ}^{QQ}(\mathbf{R}) = \mathbf{c}^I(\mathbf{R})^\dagger\,\boldsymbol{H}(\mathbf{R})\,\mathbf{c}^J(\mathbf{R}_x) \tag{6a}$$

$$H_{IK}^{QP}(\mathbf{R}) = \mathbf{C}^K(\mathbf{R}_x)^\dagger\,\boldsymbol{H}(\mathbf{R})\,\mathbf{c}^I(\mathbf{R}_x) \tag{6b}$$

$$H_{KL}^{PP}(\mathbf{R}) = \mathbf{C}^K(\mathbf{R}_x)^\dagger\,\boldsymbol{H}(\mathbf{R})\,\mathbf{c}^L(\mathbf{R}_x) \tag{6c}$$

for $I, J \leq 2$ and $K, L > 2$. Here and below the letters $I$ and $J$ will be used to denote the two degenerate states.

S1089-5639(97)00137-0 CCC: $14.00 

At a neighboring nuclear configuration, $\mathbf{R} = \delta\mathbf{R} + \mathbf{R}_x$, the Hamiltonian matrix in the CSF basis becomes

$$\boldsymbol{H}(\mathbf{R}) \cong \boldsymbol{H}(\mathbf{R}_x) + \sum_{R_\alpha} \frac{\partial \boldsymbol{H}(\mathbf{R}_x)}{\partial R_\alpha} \partial R_\alpha + 1/2 \sum_{R_\alpha, R_\beta} \delta R_\beta \frac{\partial^2 \boldsymbol{H}(\mathbf{R}_x)}{\partial R_\beta \partial R_\alpha} \delta R_\alpha \quad (7)$$

Note that the changes in $\boldsymbol{H}(\mathbf{R})$ result from both changes in the Hamiltonian operator, through the electron - nuclei attraction term, and changes in the molecular orbitals used to construct the CSFs. Thus, in the crude adiabatic basis

$$H_{II}^{QQ}(\mathbf{R}) \cong E_I(\mathbf{R}_x) + \mathbf{g}^I(\mathbf{R}_x)^\dagger \cdot \delta\mathbf{R} + {}^1/_2 \delta\mathbf{R}^\dagger \cdot \boldsymbol{\eta}^I(\mathbf{R}_x) \cdot \delta\mathbf{R} \quad (8a)$$

$$\equiv H_{II}^{0,Q} + H_{II}^{1,Q}(\mathbf{R}) + H_{II}^{2,Q}(\mathbf{R}) \quad (8b)$$

$$H_{IJ}^{QQ}(\mathbf{R}) \cong \mathbf{h}^{IJ}(\mathbf{R}_x)^\dagger \cdot \delta\mathbf{R} + {}^1/_2 \delta\mathbf{R}^\dagger \cdot \boldsymbol{\eta}^{IJ}(\mathbf{R}_x) \cdot \delta\mathbf{R} \quad (9a)$$

$$\equiv H_{IJ}^{1,Q}(\mathbf{R}) + H_{IJ}^{2,Q}(\mathbf{R}) \quad (9b)$$

where we have observed that $H_{IJ}^{QQ}(\mathbf{R}_x) = 0$, $H_{II}^{QQ}(\mathbf{R}_x) = E_I(\mathbf{R}_x)$, defined:

$$g_\alpha^I(\mathbf{R}) = \mathbf{c}^I(\mathbf{R}_x)^\dagger \frac{\partial \boldsymbol{H}(\mathbf{R})}{\partial R_\alpha} \mathbf{c}^I(\mathbf{R}_x) \quad (10a)$$

$$\eta_{\beta\alpha}^I(\mathbf{R}) = \mathbf{c}^I(\mathbf{R}_x)^\dagger \frac{\partial^2 \boldsymbol{H}(\mathbf{R})}{\partial R_\beta \partial R_\alpha} \mathbf{c}^I(\mathbf{R}_x) \quad (10b)$$

and

$$h_\alpha^{IJ}(\mathbf{R}) = \mathbf{c}^I(\mathbf{R}_x)^\dagger \frac{\partial \boldsymbol{H}(\mathbf{R})}{\partial R_\alpha} \mathbf{c}^J(\mathbf{R}_x) \quad (11a)$$

$$\eta_{\beta\alpha}^{IJ}(\mathbf{R}) = \mathbf{c}^I(\mathbf{R}_x)^\dagger \frac{\partial^2 \boldsymbol{H}(\mathbf{R})}{\partial R_\beta \partial R_\alpha} \mathbf{c}^J(\mathbf{R}_x) \quad (11b)$$

Note that at $\mathbf{R}_x$, $g_\alpha^I(\mathbf{R}_x) = \partial E_I(\mathbf{R}_x)/\partial R_\alpha$. $\mathbf{g}^I(\mathbf{R})$ and $\mathbf{h}^{IJ}(\mathbf{R})$ are readily determined using analytic gradient techniques[21] whereas the $\boldsymbol{\eta}^I$ and $\boldsymbol{\eta}^{IJ}$ are quite costly to evaluate for MCSCF/CI wave functions.

Consider, following Mead,[11] $\boldsymbol{\xi}^I(\mathbf{R})$, $\boldsymbol{\Xi}^I(\mathbf{R})$, and $\boldsymbol{H}^{RS}(\mathbf{R})$ to be expanded in a power series in $\delta\mathbf{R}$ as follows

$$\boldsymbol{\xi}^I(\mathbf{R}) \cong \boldsymbol{\xi}^{0,I}(\mathbf{R}_x) + \boldsymbol{\xi}^{1,I}(\mathbf{R}) + \boldsymbol{\xi}^{2,I}(\mathbf{R}) + ... \quad (12a)$$

$$\boldsymbol{\Xi}^I(\mathbf{R}) \cong \boldsymbol{\Xi}^{1,I}(\mathbf{R}) + \boldsymbol{\Xi}^{2,I}(\mathbf{R}) + ... \quad (12b)$$

with the expansion of $\boldsymbol{H}^{RS}$ given by eqs 8b, 9b, and (to the order required here)

$$H_{IK}^{QP}(\mathbf{R}) \cong \sum_\alpha \mathbf{c}^I(\mathbf{R}_x)^\dagger \frac{\partial \boldsymbol{H}(\mathbf{R}_x)}{\partial R_\alpha} \mathbf{C}^K(\mathbf{R}_x) \partial R_\alpha \equiv H_{IK}^{1,QP}(\mathbf{R}) \quad (13)$$

$$H_{LK}^{PP}(\mathbf{R}) \cong \mathbf{C}^L(\mathbf{R}_x)^\dagger \boldsymbol{H}(\mathbf{R}_x) \mathbf{C}^K(\mathbf{R}_x) + \sum_\alpha \mathbf{C}^L(\mathbf{R}_x)^\dagger \frac{\partial \boldsymbol{H}(\mathbf{R}_x)}{\partial R_\alpha} \mathbf{C}^K(\mathbf{R}_x) \partial R_\alpha \quad (14a)$$

$$\equiv H_{KL}^{0,P} + H_{KL}^{1,P}(\mathbf{R}) \quad (14b)$$

where we have observed that $H_{IL}^{QP}(\mathbf{R}_x) = 0$. Through second order in perturbation theory

$$[\boldsymbol{H}^{1,Q}(\mathbf{R}) - \boldsymbol{I} W_I^{(1)}(\mathbf{R})] \tilde{\boldsymbol{\xi}}^{0,I}(\mathbf{R}) = \mathbf{0} \quad (15a)$$

$$\boldsymbol{\Xi}^{1,I}(\mathbf{R}) = [\boldsymbol{I} E_I(\mathbf{R}_x) - \boldsymbol{H}^{0,P}]^{-1} \boldsymbol{H}^{1,PQ}(\mathbf{R}) \tilde{\boldsymbol{\xi}}^{0,I}(\mathbf{R}) \quad (15b)$$

and

$$[\bar{\boldsymbol{H}}^{2,Q}(\mathbf{R}) - W_I^{(2)}(\mathbf{R})] \tilde{\boldsymbol{\xi}}^{0,I}(\mathbf{R}) + [\boldsymbol{H}^{1,Q}(\mathbf{R}) - W_I^{(1)}(\mathbf{R})] \tilde{\boldsymbol{\xi}}^{1,I}(\mathbf{R}) = \mathbf{0} \quad (16)$$

which implies

$$\tilde{\boldsymbol{\xi}}^{1,I}(\mathbf{R}) = \tilde{\boldsymbol{\xi}}^{0,J}(\mathbf{R}) [\tilde{\boldsymbol{\xi}}^{0,J}(\mathbf{R})^\dagger \bar{\boldsymbol{H}}^{2,Q}(\mathbf{R}) \tilde{\boldsymbol{\xi}}^{0,I}(\mathbf{R})] / [W_I^{(1)}(\mathbf{R}) - W_J^{(1)}(\mathbf{R})] \quad (17a)$$

$$W_I^{(2)}(\mathbf{R}) = \tilde{\boldsymbol{\xi}}^{0,I}(\mathbf{R})^\dagger \bar{\boldsymbol{H}}^{2,Q}(\mathbf{R}) \tilde{\boldsymbol{\xi}}^{0,I}(\mathbf{R}) \quad (17b)$$

where

$$\bar{\boldsymbol{H}}^{2,Q}(\mathbf{R}) = \boldsymbol{H}^{2,Q}(\mathbf{R}) + \boldsymbol{H}^{1,QP}(\mathbf{R}) [\boldsymbol{I} E_I(\mathbf{R}_x) - \boldsymbol{H}^{0,P}]^{-1} \boldsymbol{H}^{1,QP}(\mathbf{R}) \quad (18)$$

Note that the geometry-independent $\boldsymbol{\xi}^{0,I}$ become the geometry-dependent $\tilde{\boldsymbol{\xi}}^{0,I}(\mathbf{R})$ by requiring eq 15a.

It is useful at this point to define, the $g$-$h(\mathbf{R}_x)$ plane by the vectors, $\mathbf{g}^{IJ}(\mathbf{R}_x) \equiv \mathbf{g}^J(\mathbf{R}_x) - \mathbf{g}^I(\mathbf{R}_x)$ and $\mathbf{h}^{IJ}(\mathbf{R}_x)$, and its orthogonal complement, $g$-$h^\perp(\mathbf{R}_x)$, a space of dimension $N^{\text{int}} - 2$, where $N^{\text{int}}$ is the number of internal degrees of freedom. From eqs 8, 9, and 15a it is seen that only in the $g$-$h$ plane is the degeneracy lifted at first order in perturbation theory.

Using eqs 8−11 in eq 15a gives

$$\begin{pmatrix} -\Delta H_{IJ}^{1,Q} & H_{IJ}^{1,Q} \\ H_{IJ}^{1,Q} & \Delta H_{IJ}^{1,Q} \end{pmatrix} \begin{pmatrix} \tilde{\xi}_1^{0,I} \\ \tilde{\xi}_2^{0,I} \end{pmatrix} = \begin{pmatrix} -gx & h_x x + h_y y \\ h_x x + h_y y & gx \end{pmatrix} \begin{pmatrix} \tilde{\xi}_1^{0,I} \\ \tilde{\xi}_2^{0,I} \end{pmatrix} = \epsilon_I \begin{pmatrix} \tilde{\xi}_1^{0,I} \\ \tilde{\xi}_2^{0,I} \end{pmatrix} \quad (19)$$

where $x = \rho \cos\theta$ [$y = \rho \sin\theta$] is the displacement along $\tilde{\mathbf{g}}^{IJ}(\mathbf{R}_x)$ [$\bar{\mathbf{g}}^{IJ}(\mathbf{R}_x)$], a unit vector in nuclear coordinate space parallel [perpendicular] to $\mathbf{g}^{IJ}(\mathbf{R}_x)$ in the $g$-$h(\mathbf{R}_x)$ plane; $\mathbf{z}$ represents the internal nuclear coordinates in the $g$-$h^\perp(\mathbf{R}_x)$ manifold,

$$\Delta H_{IJ}^Q(\mathbf{R}) \equiv (H_{JJ}^{QQ}(\mathbf{R}) - H_{II}^{QQ}(\mathbf{R}))/2 \cong \Delta H_{IJ}^{1,Q}(\mathbf{R}) + \Delta H_{IJ}^{2,Q}(\mathbf{R}) \quad (20a)$$

$$W_I^1(\mathbf{R}) = \epsilon_I(\rho,\theta) + H(\rho,\theta,\mathbf{z};\mathbf{s}) \equiv \epsilon_I(\rho,\theta) + s_x x + s_y y + \mathbf{s}_z^\dagger \cdot \mathbf{z} \quad (20b)$$

$$g = |\mathbf{g}^{IJ}(\mathbf{R}_x)|/2 \quad (21)$$

$$h_x = \mathbf{h}^{IJ}(\mathbf{R}_x) \cdot \tilde{\mathbf{g}}^{IJ}(\mathbf{R}_x) \quad (22a)$$

$$h_y = \mathbf{h}^{IJ}(\mathbf{R}_x)\cdot\bar{\mathbf{g}}^{IJ}(\mathbf{R}_x) \tag{22b}$$

$$s_x = [\mathbf{g}^I(\mathbf{R}_x) + \mathbf{g}^J(\mathbf{R}_x)]\cdot\bar{\mathbf{g}}^{IJ}(\mathbf{R}_x)/2 \tag{23a}$$

$$s_y = [\mathbf{g}^I(\mathbf{R}_x) + \mathbf{g}^J(\mathbf{R}_x)]\cdot\bar{\mathbf{g}}^{IJ}(\mathbf{R}_x)/2 \tag{23b}$$

and $\mathbf{s}_z$ is the projection of $[\mathbf{g}^I(\mathbf{R}_x) + \mathbf{g}^J(\mathbf{R}_x)]/2$ onto the $g$-$h^\perp(\mathbf{R}_x)$ manifold. Equivalent results are obtained if $\mathbf{h}^{IJ}(\mathbf{R}_x)$ is taken as the $x$-axis.

Equation 19 can be transformed into a more convenient form by defining $q(\theta)$ and $\lambda(\theta)$

$$q(\theta)^2 = g^2\cos^2\theta + (h_x\cos\theta + h_y\sin\theta)^2 \equiv g^2\cos^2\theta + h^2\sin^2(\theta+\alpha) \tag{24a}$$

$$\cos\lambda = g/q\ cos\ \theta \qquad \sin\lambda = h/q\sin(\theta+\alpha) \tag{24b}$$

so that eq 19 becomes:

$$\rho q\begin{pmatrix}-\cos\lambda & \sin\lambda\\ \sin\lambda & \cos\lambda\end{pmatrix}\begin{pmatrix}\tilde{\xi}_1^{0,I}\\ \tilde{\xi}_2^{0,I}\end{pmatrix} = \epsilon_I\begin{pmatrix}\tilde{\xi}_1^{0,I}\\ \tilde{\xi}_2^{0,I}\end{pmatrix} \tag{25}$$

The eigenvalues and eigenfunctions (in the CSF basis) of eq 25 are (for $I = K^-$ and $J = K^+$)

$$\epsilon_{K^\pm} = \pm\rho q(\theta) \tag{26a}$$

$$\begin{pmatrix}\tilde{\boldsymbol{\xi}}^{0,K^-}(\theta)\\ \tilde{\boldsymbol{\xi}}^{0,K^+}(\theta)\end{pmatrix} = \begin{pmatrix}\cos\lambda(\theta)/2 & -\sin\lambda(\theta)/2\\ \sin\lambda(\theta)/2 & \cos\lambda(\theta)/2\end{pmatrix}\begin{pmatrix}\mathbf{c}^1(\mathbf{R}_x)^\dagger\ \boldsymbol{\psi}(\mathbf{r};\mathbf{R})\\ \mathbf{c}^2(\mathbf{R}_x)^\dagger\ \boldsymbol{\psi}(\mathbf{r};\mathbf{R})\end{pmatrix} \tag{26b}$$

where as the notation in eq 26b indicates the **R** dependence of the CSFs, $\boldsymbol{\psi}(\mathbf{r};\mathbf{R})$, is subordinate to that induced by the perturbation expansion.

Thus the parameters in eqs 21−23, which are readily evaluated using analytic gradient techniques, determine the topology of the potential energy surfaces in the immediate vicinity of a conical intersection. We will refer to $\rho$, $\theta$, and **z** as canonical coordinates and $\mathbf{g}^{IJ}(\mathbf{R}_x)$, $\mathbf{h}^{IJ}(\mathbf{R}_x)$, and $\mathbf{s}(\mathbf{R}_x)$ as the characteristic parameters. It is important to observe that $\mathbf{c}^I(\mathbf{R}_x)$ and $\mathbf{c}^J(\mathbf{R}_x)$ are defined up to a one parameter rotation so that only the $g$-$h$ plane is uniquely defined. Thus while the definition of the $x$-axis is fixed once $\mathbf{c}^I(\mathbf{R}_x)$ and $\mathbf{c}^J(\mathbf{R}_x)$ are defined, it is not unique and the parameters $\mathbf{g}^{IJ}(\mathbf{R}_x)$, $\mathbf{h}^{IJ}(\mathbf{R}_x)$, and $\mathbf{s}(\mathbf{R}_x)$ are not unique either. This point will be considered further in section III.

**B. Geometric Phase Effect.** From eqs 24 and 26b it is seen that when the electronic wave functions are transported around a circle in the $g$-$h$ plane, that is when $\theta$ increases by $2\pi$, $\lambda$ increases by $2\pi$ but since $\lambda/2$ only increases by $\pi$, $\tilde{\boldsymbol{\xi}}^{0,K^\pm} \rightarrow -\tilde{\boldsymbol{\xi}}^{0,K^\pm}$. This is the geometric phase effect.[3,22,5] If the (infinitesimal) closed loop does not contain a point of conical intersection, nondegenerate perturbation theory suffices and a sign change on transporting the electronic wave function around a closed loop is not possible since the zeroth-order component can never vanish.[4]

**C. Derivative Couplings.** In conventional uses of degenerate perturbation theory, lower order wave functions are used to determine higher order energies. Mead observed[11] that in the presence of a conical intersection higher order energies of *one* potential energy surface could be used to infer information about lower order wave functions for both states and hence about the energetics on the companion surface and the derivative couplings; see for example eqs 17a and 17b. Here we focus on the derivative couplings since knowledge of their limiting form at a conical intersection can be used to assess the precision of the numerical procedures used in their evaluation.

$f_\alpha^{JI}(\mathbf{R})$, consists of two contributions

$$f_\alpha^{JI}(\mathbf{R}) = {}^{\mathrm{CI}}f_\alpha^{JI}(\mathbf{R}) + {}^{\mathrm{CSF}}f_\alpha^{JI}(\mathbf{R}) \tag{27}$$

where the CI contribution is given by

$${}^{\mathrm{CI}}f_\alpha^{JI}(\mathbf{R}) = \tilde{\xi}^J(\mathbf{R})^\dagger\left(\frac{\partial}{\partial R_\alpha}\tilde{\xi}^I(\mathbf{R})\right) + \Xi^J(\mathbf{R})^\dagger\left(\frac{\partial}{\partial R_\alpha}\Xi^I(\mathbf{R})\right) \tag{28a}$$

and the CSF contribution has the form

$${}^{\mathrm{CSF}}f_\alpha^{JI}(\mathbf{R}) = \sum_{\lambda,\mu} c_\lambda^J(\mathbf{R})\left\langle\psi_\lambda(\mathbf{r};\mathbf{R})\left|\frac{\partial}{\partial R_\alpha}\psi_\mu(\mathbf{r};\mathbf{R})\right\rangle_{\mathbf{r}} c_\mu^I(\mathbf{R}) \right. \tag{28b}$$

In the vicinity of a conical intersection the CI portion of the derivative coupling is preeminent,[10] although both contributions will be evaluated in the MCSCF/CI treatment.

The first term in eq 28a contains the first nonvanishing contribution to the derivative coupling. The form of this term can be deduced from eqs 17a, 17b, and 26b. In the development that follows we restrict our attention to triatomic molecules for which the orientation of the $g$-$h$ plane is constant along the crossing seam. This approximation is valid for the $1^1A'$ - $2^1A'$ seam in $HeH_2$ and has been used previously by Kendrick and Pack in their treatment of the geometric phase effect in $O_2H$.[23−25] With this assumption and since $\boldsymbol{H}(\mathbf{R})$ is real-valued

$$\bar{\boldsymbol{H}}^{2,Q}(\mathbf{R}) = \rho[A(\theta,z)\,\boldsymbol{\sigma}_z + B(\theta,z)\,\boldsymbol{\sigma}_x] \tag{29}$$

where $\boldsymbol{\sigma}_x$ and $\boldsymbol{\sigma}_z$ are the Pauli matrices,[26]

$$A(\rho,\theta,z) = z(a_1\cos\theta + a_2\sin\theta) + \rho(a_3\cos^2\theta + a_4\sin^2\theta + a_5\sin\theta\cos\theta) \tag{30a}$$

$$B(\rho,\theta,z) = z(b_1\cos\theta + b_2\sin\theta) + \rho(b_3\cos^2\theta + b_4\sin^2\theta + b_5\sin\theta\cos\theta) \tag{30b}$$

and the contribution from a unit (2 × 2) matrix has been ignored. Transforming to the $\tilde{\xi}^{0,K^\pm}$ basis by noting $\tilde{\boldsymbol{\sigma}}_x \equiv \boldsymbol{u}(\lambda)^\dagger\,\boldsymbol{\sigma}_x\,\boldsymbol{u}(\lambda) = -\sin\lambda\,\boldsymbol{\sigma}_z + \cos\lambda\,\boldsymbol{\sigma}_x$ and $\tilde{\boldsymbol{\sigma}}_z = \sin\lambda\,\boldsymbol{\sigma}_x + \cos\lambda\,\boldsymbol{\sigma}_z$, where $\boldsymbol{u}(\lambda)$ is the 2 × 2 matrix in eq 26b gives

$$\bar{\boldsymbol{H}}^{2,Q} = \rho[(A\cos\lambda - B\sin\lambda)\boldsymbol{\sigma}_z + (A\sin\lambda + B\cos\lambda)\boldsymbol{\sigma}_x] \tag{31}$$

so that

$$\tilde{\boldsymbol{\xi}}^I \cong \tilde{\boldsymbol{\xi}}^{0,I} + \frac{(A(\rho,\theta,z)\sin\lambda(\theta) + B(\rho,\theta,z)\cos\lambda(\theta))}{2\,q(\theta)}\tilde{\boldsymbol{\xi}}^{0,J} \tag{32a}$$

$$\tilde{\boldsymbol{\xi}}^J \cong \tilde{\boldsymbol{\xi}}^{0,J} - \frac{(A(\rho,\theta,z)\sin\lambda(\theta) + B(\rho,\theta,z)\cos\lambda(\theta))}{2\,q(\theta)}\tilde{\boldsymbol{\xi}}^{0,I} \tag{32b}$$

Noting, from eq 26b that

$$\tilde{\boldsymbol{\xi}}^{0,J}(\theta)^\dagger\frac{\partial}{\partial\lambda}\tilde{\boldsymbol{\xi}}^{0,I}(\theta) = 1/2 \tag{33a}$$

$$\tilde{\boldsymbol{\xi}}^{0,J}(\theta)^\dagger\frac{\partial}{\partial\tau}\tilde{\boldsymbol{\xi}}^{0,I}(\theta) = 0 \qquad \tau = \rho, z \tag{33b}$$

gives for the first nonvanishing terms

$$^{\mathrm{CI}}f_{\theta}^{JI}(\mathbf{R}) = 1/2\,\frac{\mathrm{d}\lambda}{\mathrm{d}\theta} = 1/2\frac{|\mathbf{g}^{IJ}/2|\sin(\alpha+\pi/2)|\mathbf{h}^{IJ}|}{q^2(\theta)} \quad (34a)$$

$$^{\mathrm{CI}}f_{\rho}^{JI}(\mathbf{R}) = m_1(\theta)/q(\theta) \quad (34b)$$

$$^{\mathrm{CI}}f_{z}^{JI}(\mathbf{R}) = m_2(\theta)/q(\theta) \quad (34c)$$

where

$$m_1(\theta) = \bar{c}_1\cos(\lambda+\bar{\gamma}_1) + [(\bar{a}_{11}\cos 2\theta + \bar{a}_{21}\sin 2\theta)\sin\lambda + (\bar{b}_{11}\cos 2\theta + \bar{b}_{21}\sin 2\theta)\cos\lambda] \quad (35a)$$

$$m_2(\theta) = \bar{a}_2\cos(\theta-\bar{\alpha}_1)\sin\lambda + \bar{b}_2\cos(\theta-\bar{\beta}_1)\cos\lambda \quad (35b)$$

and the "barred" constants can be obtained from the $a_i$ and $b_i$ in eq 30 by straightforward algebra. If $\mathbf{g}^{IJ}$ and $\mathbf{h}^{IJ}$ are perpendicular and of equal length, the right hand side of eq 34a is 1/2. The $\rho \rightarrow 0$ limit of $f_z^{JI}(\rho,\theta,z)$ obtained here in the absence of spatial symmetry differs qualitatively from the symmetry-determined $X_3$ case for which $f_z^{JI}(\rho,\theta,z) \rightarrow 0$ as $\rho \rightarrow 0$.[11]

**D. The Circulation of the Derivative Coupling.** From eq 34a, the circulation of $\mathbf{f}^{IJ}(\mathbf{R})$ along an infinitesimal loop in the *g-h* plane surrounding $\mathbf{R}_x$ is given by:

$$\oint_C \mathbf{f}^{IJ}(\mathbf{R})\cdot\mathrm{d}\mathbf{R} = \int_0^{2\pi} 1/2\,\mathrm{d}\lambda = \pi \quad (36)$$

However, if $C$ does not contain a point of conical intersection, then the circulation of $\mathbf{f}^{IJ}(\mathbf{R})$ approaches 0 as $\rho$ decreases to zero. Thus the line integral in eq 36 can be used to prove the existence of a conical intersection point. Below it will be convenient to denote a circle in the *g-h* plane with origin O and radius $\rho$, by $C(\rho,\mathrm{O})$ and to denote the set of values of a function $w(\mathbf{R})$ on $C$ by $w[C]$.

The inverse of the transformation in eq 26b provides a transformation to a basis that removes the singularity in the derivative coupling. Thus the angle $\lambda(\theta)$ can be used as the rotation angle of a transformation to approximate diabatic states. This transformation can be used together with *ab initio* energies and derivative couplings to extend the standard two-dimensional treatment of a Jahn-Teller problem[27] to non $C_{3v}$ molecules. In the present approach the interstate coupling would consist of both potential and derivative coupling contributions. The residual derivative coupling would be nonsingular but would be more than just the nonremovable part, the portion of the derivative coupling that cannot be removed by a transformation to approximate diabatic states.[28] In this regard note that the quantity

$$\Delta(C) \equiv \oint_C \mathbf{f}^{IJ}(\mathbf{R})\cdot\mathrm{d}\mathbf{R} - \kappa(C) \quad (37)$$

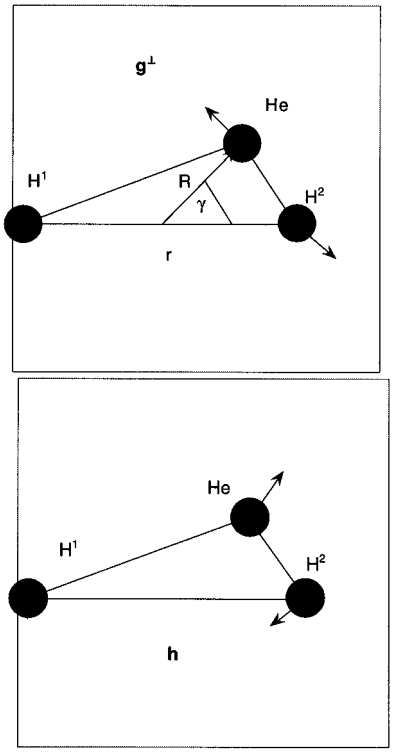


**Figure 1.** Unit vectors in the directions $\mathbf{h}^{IJ}(\mathbf{R}_{\mathrm{mex}})$ and $\mathbf{g}^{IJ}(\mathbf{R}_{\mathrm{mex}})^{\perp}$ (the component of $\mathbf{g}^{IJ}(\mathbf{R}_{\mathrm{mex}})$ in the *g-h* plane perpendicular to $\mathbf{h}^{IJ}(\mathbf{R}_{\mathrm{mex}})$), represented in terms of atomic displacements. Also displayed are the Jacobi coordinates, *R*, *r*, $\gamma$.

where $\kappa(C) = 0[\pi]$ if $C$ contains no [one] point of conical intersection represents a measure of the nonremovable part of the derivative coupling.[28,29]

## III. The $1^1A'$ - $2^1A'$ Seam of Conical Intersections in $HeH_2$

For the triatomic molecule $HeH_2$ molecular geometries will be specified by the Jacobi coordinates: *r* the $H^1-H^2$ distance, *R* the distance between He and the center of mass of $H_2$, and $\gamma$ the angle between the line segments corresponding to *R* and *r*, such that $\gamma = 90°$ for $C_{2v}$ geometries. See Figure 1. The adiabatic electronic wave functions are based on a second-order CI expansion[30] using a four $a'$ orbital active space and He[7s2p1d], H[6s3p] basis sets as described in detail previously.[14] This level of treatment was previously used to determine points, $\mathbf{R}_x$, on the $1^1A'$ - $2^1A'$ seam of conical intersections which was parameterized by *r*, that is $\mathbf{R}_x(r) \equiv [R(r), \gamma(r), r]$. Here two $\mathbf{R}_x(r)$ will be considered, the minimum energy crossing point $\mathbf{R}_{\mathrm{mex}} \equiv \mathbf{R}_x(3.7294)$ and $\mathbf{R}_x(4.0)$. In this work the *x*-axis is taken along $\mathbf{h}^{IJ}$ so that Table 1 reports *R*, $\gamma$, *r*, **g**, *h*, and **s** for these two points. Figure 1 depicts $\mathbf{g}^{IJ}(\mathbf{R}_{\mathrm{mex}})$ and

**TABLE 1: $HeH_2$ $1^1A'$ - $2^1A'$ Crossing Seam[a]**

| *R* ($a_0$) | *r* ($a_0$) | *E* (kcal/mol) | *h* (au) | **g** (au) | **s** (au) |
|---|---|---|---|---|---|
| | $\gamma$ (deg) | $\Delta E$ ($cm^{-1}$) | | | |
| | | | $\mathbf{R}_{\mathrm{mex}} = \mathbf{R}_x(3.73)$ | | |
| 1.5662 | 3.7294 | −38.141 | 0.0879 | 0.0181 | −0.0558 |
| | 44.373 | 0.020 | | 0.1630 | 0.2051 |
| | | | | | 0.0002 |
| | | | $\mathbf{R}_x(4.0)$ | | |
| 1.6601 | 4.0000 | −36.891 | 0.0753 (0.1244) | 0.0135 (−0.0821) | −0.0069 (−0.2178) |
| | 40.316 | 0.021 | | 0.1607 (0.0972) | −0.2336 (0.0849) |
| | | | | | 0.0070 (0.0070) |

[a] $\Delta E = E_{2^1A'} - E_{1^1A'}$. $E = E_{1^1A'} \sim E_{2^1A'}$ relative to $E_{2^1A'} = -3.650\,107$ au at $r = 2.393$ $a_0$, $R = 50$ $a_0$. For $\mathbf{R}_x(4.0)$ the second parameter set is given parenthetically. For **g** and **s**, *x*,*y* and *x*,*y*,*z* components are given down the corresponding column.

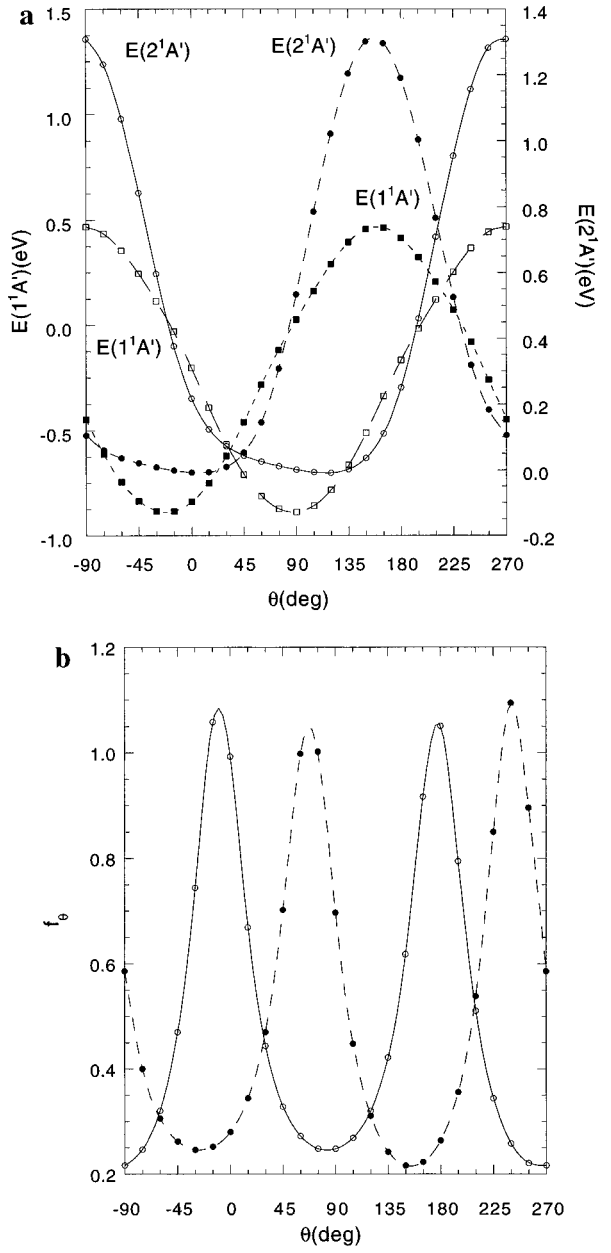


**Figure 2.** $E_{1^1A'}[C(\rho,\mathbf{R}_x(4.0))]$, $E_{2^1A'}[C(\rho,\mathbf{R}_x(4.0))]$, (a), and $f_\theta[C(\rho,\mathbf{R}_x(4.0))]$, (b), from MCSCF/CI wave functions for $\rho = 0.1$ with $C(\rho,\mathbf{R}_x(4.0))$ obtained from two distinct parameter sets in Table 1. Open markers represent the first parameter set, filled markers the second (parenthetical) parameter set. Energies are in eV relative to $E_{1^1A'}(\mathbf{R}_x(4.0)) = -3.710\,887$ au.

$\mathbf{h}^{IJ}(\mathbf{R}_{mex})$. For $\mathbf{R}_x(4.0)$ two sets of characteristic parameters are reported. Note that although the $(\mathbf{c}^I(\mathbf{R}_x), \mathbf{c}^J(\mathbf{R}_x))$ pairs associated with these two sets of parameters are related by a rotation, the corresponding $(\mathbf{g}^{IJ}(\mathbf{R}_x), \mathbf{h}^{IJ}(\mathbf{R}_x))$ pairs are not so related.

**A. Rotational Invariance of Conical Intersection Parameters.** As observed above while the *g*-*h* plane is uniquely defined, the vectors $\mathbf{g}^{IJ}$ and $\mathbf{h}^{IJ}$, and hence the characteristic parameters for the conical intersection, are arbitratry up to a one-parameter rotation. One measure of the precision of the numerical procedures used to determine the characteristic parameters is provided by the consistency of two sets of characteristic parameters at a particular point on the surface of conical intersection. Table 1 reports two such sets of characteristic parameters for $\mathbf{R}_x(4.0)$. The equivalence of these parameter sets can be demonstrated in many ways. Figure 2a,b provides one such demonstration reporting $E_I[C(0.1,\mathbf{R}_x(4.0))]$ and $f_\theta[C(0.1,\mathbf{R}_x(4.0))]$, respectively obtained from MCSCF/CI

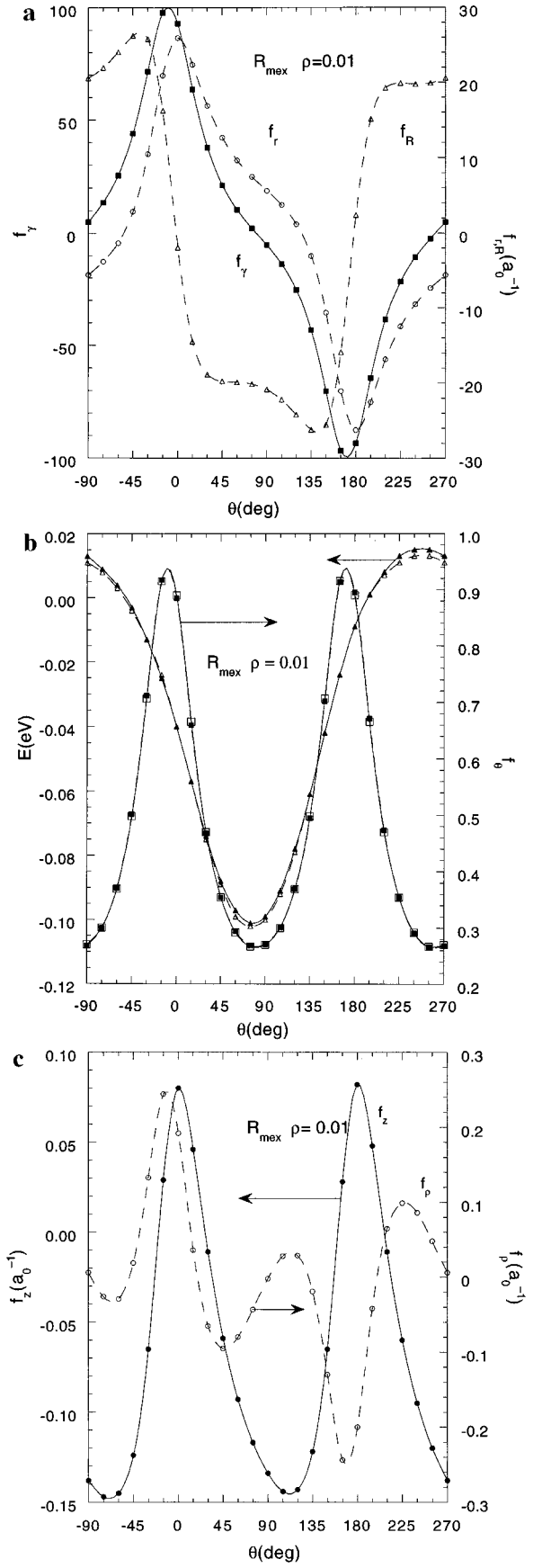


**Figure 3.** (a) $f_\tau[C(\rho,\mathbf{R}_{mex})]$, $\tau$ = r, R, $\gamma$ for $\rho = 0.01$, from *ab initio* calculations. (b) $E_{1^1A'}[C(\rho,\mathbf{R}_{mex})]$, triangular markers, and $f_\theta[C(\rho,\mathbf{R}_{mex})]$, square markers, for $\rho = 0.01$. Filled markers are from *ab initio* calculations; open markers are from perturbation theory using the parameter set in Table 1. (c) $f_\tau[C(\rho,\mathbf{R}_{mex})]$, $\tau = z$ (filled circles), $\rho$ (open circles) for $\rho = 0.01$ from *ab initio* calculations.

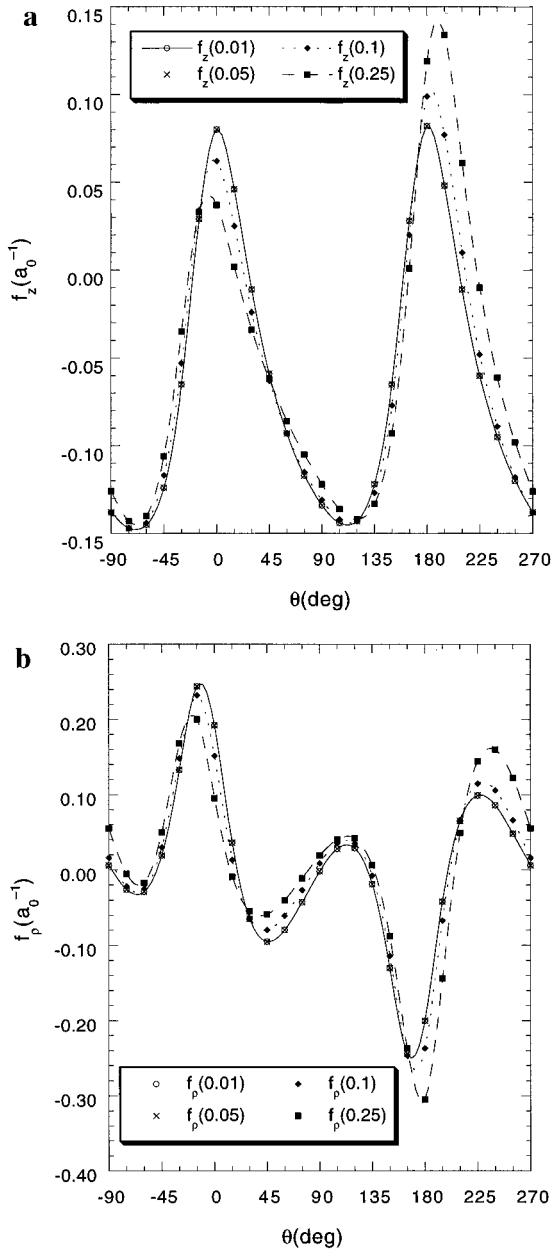


**Figure 4.** Convergence of $f_\tau[C(\rho,\mathbf{R}_{mex})]$ from *ab initio* calculations for $\rho = 0.25$ (solid squares), 0.1 (solid circles), 0.05 (×), and 0.01 (open circles); (a) $\tau = z$, (b) $\tau = \rho$.

wave functions with $C(0.1,\mathbf{R}_x(4.0))$ determined from these two sets of characteristic parameters. Here and below the *JI* superscript on the derivative coupling will be suppressed. From this figure it is clear that the solid curves (first parameter set) can be brought into coincidence with the dashed curves (second parameter set) by a shift of −120°.

**B. Energies and Derivative Couplings: Comparison with the Linear Expansion.** We next turn to the energetics and derivative couplings in the immediate vicinity of a conical intersection, using $\mathbf{R}_{mex}$. Figure 3 considers $\rho = 0.01$. Figure 3a reports $f_\tau[C(0.01,\mathbf{R}_{mex})]$, $\tau = r, R, \gamma$. The large values of the derivative couplings in this Jacobi representation are consistent with the small value of $\rho$. The size of the derivative couplings in this representation suggests that numerical problems may be obtained when transforming to the "canonical", $z, \rho, \theta$, representation. However this is emphatically not the case. Figure 3b reports $E_{1^1A'}[C(0.01,\mathbf{R}_{mex})]$ and $f_\theta[C(0.01,\mathbf{R}_{mex})]$ determined from MCSCF/CI wave functions and from eqs 20b, 26a and 34a using the parameter set from Table 1.

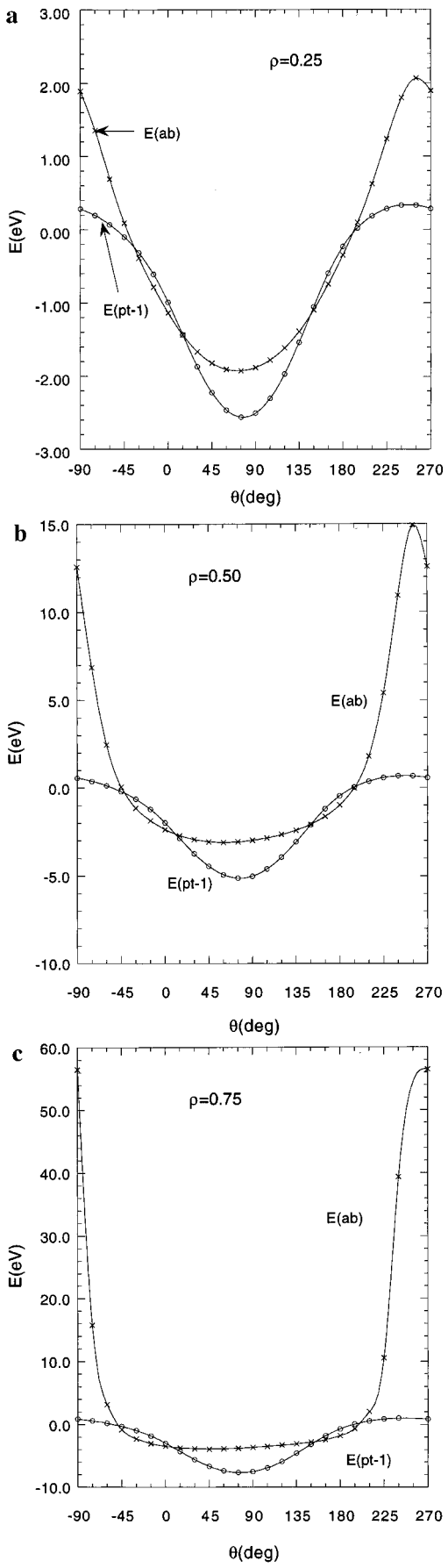


**Figure 5.** $E_{1^1A'}[C(\rho,\mathbf{R}_{mex})]$ for $\rho = 0.25$ (a), 0.50 (b), and 0.75 (c) as determined from *ab initio* calculations, $E$(ab), and from eqs 20 and 26a, $E$(pt-1).

$E_{1^1A'}[C(0.01,\mathbf{R}_{mex})]$ and $f_\theta[C(0.01,\mathbf{R}_{mex})]$ calculated from MCSCF/CI wave functions are *virtually identical* with those obtained from first-order perturbation theory. Figure 3c reports $f_\rho[C(0.01,\mathbf{R}_{mex})]$ and $f_z[C(0.01,\mathbf{R}_{mex})]$ determined from *ab initio* calculations. On the basis of the results in Figure 3b, and as discussed below, these values are expected to be close to their $\rho = 0$ values. While the specifics of the $\theta$-dependence of $f_\tau[C]$, $\tau = \rho, z$ require second-derivative information—more expensive to obtain than the derivative coupling—it is worth noting that $f_\rho[C]$ has higher frequency oscillations than $f_z[C]$ which is consistent with the functional forms in eqs 34b and 34c.

The $\rho$-dependence of $f_\tau[C]$ is considered in more detail in Figure 4. This figure, which reports $f_\tau[C(\rho,\mathbf{R}_{mex})]$ for $\rho = 0.25$ (solid squares), 0.1 (solid circles), 0.05 (x), and 0.01 (open circles), illustrates that $f_\tau[C(\rho,\mathbf{R}_{mex})]$, $\tau = z$ (Figure 4a), and $\tau = \rho$ (Figure 4b) in fact converge to a finite limit in a well-behaved manner as $\rho \rightarrow 0$. In this regard observe that for $\rho \leq 0.05$ the results are indistinguishable.

The excellent agreement between the perturbation theory and the MCSCF/CI-based results in the immediate vicinity of the conical intersection serves to confirm the precision of the numerical techniques[8−10] used to evaluate the derivative couplings in this most challenging, yet essential, region of coordinate space.

**C. Energetics and Derivative Couplings along Closed Loops in the *g*-*h* Plane.** We now consider $E_{1^1A'}[C(\rho,\mathbf{R}_{mex})]$ and $f_\tau[C(\rho,\mathbf{R}_{mex})]$ for $\rho = 0.25, 0.50, 0.75$. These calculations address two issues of practical importance for the dynamics of reaction 2, the energy of the lower adiabatic potential energy surface relative to that of the conical intersection, and the nonremovable part of the derivative coupling. As discussed by Mead[1] and subsequently by Kupperman[2] when the total energy available to a system exceeds $E_I[C]$, *adiabatic* nuclear dynamics on that potential energy surface may be altered by the geometric phase effect. In this regard parts a - c of Figure 5 evince significant barriers along such closed loops at $\theta \sim -90°$ for $\rho = 0.25$, 0.50, and 0.75, respectively, while particularly favorable energetics occur at $\theta \sim 90°$. The $\rho = 0.25$ results suggest the following interpretation. $W_1[C]$ is the sum of two contributions, $H(\rho,\theta,z;\mathbf{s})$ and $-q(\theta)\rho$ (always negative); see eqs 20b and 26a. Thus the large value of $s_y$, compared with **g** and *h* precludes a low-energy path surrounding $\mathbf{R}_{mex}$. This interpretation is also supported by the small $\rho$ results in Figure 3b. A similar situation is found for $\mathbf{R}_x(4.0)$. See Figure 2a.

Additional insight in this regard is provided by Figure 6 which depicts the nuclear configurations for $\rho = 0.5$ and $\theta = \pm 90°$. From this figure it is seen that the barrier ($\theta \sim -90°$) occurs for configurations characterized as H + HeH and results from the small value of $R(He-H^2)$. This is, in turn, a consequence of the small value of $R(He-H^2)$ at $\mathbf{R}_{mex}$, $R(He-H^2) = 1.05$ $a_0$. Note from Figure 1 that $\theta = \pm 90°$ is largely an $He-H^2$ stretch. Note too that HeH is not bound in its ground electronic state.[31] The favorable energetics occur for triangular H−He−H configurations. Quite the opposite situation was found for $H_3$.[32] For the $1^2A'$ ground state of $H_3$, the maximum of $E_{1^2A'}[C(0.5,\mathbf{R}_{mex})]$ is less than $E_{1^2A'}(\mathbf{R}_{mex})$ by approximately 1.3 eV. In this case $s_x = s_y = 0$, and the H + $H_2$ configuration is energetically favorable.

This analysis suggests that the energetics in the vicinity of a conical intersection can be profitably analyzed in terms of the characteristic parameters presented in eqs 21−23. Future studies will attempt to better understand the relationships among $q(\theta)$, **s**, the configurations along $C(\rho,\mathbf{R}_{mex})$, and hence $E_I[C(\rho,\mathbf{R}_{mex})]$.

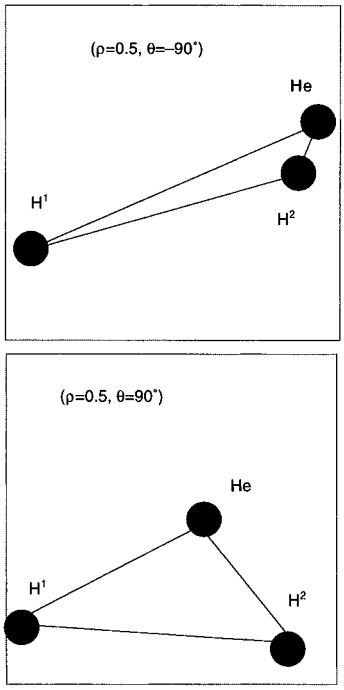


**Figure 6.** Nuclear configurations corresponding to the low-energy region (lower panel), $\theta = 90°$, $R(He-H^1) = 3.06$ $a_0$, $R(He-H^2) = 2.02$ $a_0$, and $R(H^1-H^2) = 4.03$ $a_0$, and high-energy region (upper panel), $\theta = -90°$, $R(He-H^1) = 3.32$ $a_0$, $R(He-H^2) = 0.653$ $a_0$, and $R(H^1-H^2) = 3.45$ $a_0$ of $E_{1^1A'}[C(\rho = 0.50,\mathbf{R}_{mex})]$.

Evaluation of $\Delta(C)$, eq 37, provides a quantitative measure of the size of the nonremovable part of the derivative coupling. Near $\mathbf{R}_{mex}$ we find $[\rho, \Delta(\rho, \mathbf{R}_{mex})] = [0.005, 0.0001\pi]$, $[0.01, 0.0001\pi]$, $[0.05, 0.0004\pi]$, $[0.1, 0.0014\pi]$, $[0.25, 0.0094\pi]$, $[0.5, 0.0485\pi]$, $[0.75, 0.0513\pi]$. Note that the calculation of the derivative coupling is tractable even for $\rho = 0.005$. The values of $\Delta(C)$, which represent a deviation of at most 9° from the removable result, show that the nonremovable part of the derivative coupling is small even for $\rho = 0.75$ $a_0$, for which $E_{1^1A'}$ is, in turn, quite large for a significant portion $C$. See Figure 5c. Consequently it should be possible to construct diabatic states to an excellent approximation for this system. This question will be considered in detail in a future work in which energy and derivative coupling surfaces will be reported for the $1^1A'$ and $2^1A'$ states. An analysis of the nonremovable part of the derivative coupling for $H_3$ analogous to that discussed above can be found in ref 29. A formal analysis of the derivative couplings in $H_3$ can be found in ref 11.

## IV. Summary and Conclusions

The derivative couplings and the energetics in the vicinity of a conical intersection have been considered. Using degenerate perturbation theory it is shown that previously developed analytic gradient based techniques provide a reliable method for evaluating derivative couplings in the immediate vicinity of a conical intersection. These numerical procedures can therefore be used to determine an entire surface of derivative couplings that will reliably merge into regions of conical intersections. The analysis yields an approximate diabatization scheme that can be used in conjunction with *ab initio*, derivative couplings, and potential energy surfaces to extend the standard two-dimensional treatment of the dynamic Jahn-Teller effect to molecules that do not possess $C_{3v}$ symmetry.

The $1^1A'$ - $2^1A'$ seam of conical intersections in $HeH_2$ was considered. It was shown that a barrier along closed loops surrounding points on the seam of conical intersections is

attributable to the energetically unfavorable H + HeH structure and that this barrier is reflected in the characteristic parameters for the conical intersection determined from analytic gradient techniques. It will therefore be interesting to investigate the relation between energetics in the vicinity of conical intersections and the characteristic parameters for molecules for which the A + BC structure is more energetically favorable.

**Acknowledgment.** The calculations reported in this work were performed on DRY's IBM RISC 6000/workstations purchased with funds provided by AFOSR Grant AFOSR 90-0051, NSF Grant CHE 91-03299, and DOE-BES Grant DE-FG092-91-ER14189.

## References and Notes

(1) Mead, C. A. *J. Chem. Phys.* **1980**, *72*, 3839.
(2) Kuppermann, A.; Wu, Y.-S. M. *Chem. Phys. Lett.* **1993**, *205*, 577.
(3) Longuet-Higgins, H. C. *Adv. Spectrosc.* **1961**, *2*, 429.
(4) Mead, C. A.; Truhlar, D. G. *J. Chem. Phys.* **1979**, *70*, 2284.
(5) Berry, M. V. *Proc. R. Soc. London, Ser. A* **1984**, *392*, 45−57.
(6) Mead, C. A. *Rev. Mod. Phys.* **1992**, *64*, 51.
(7) Yarkony, D. R. *Rev. Mod. Phys.* **1996**, *68*, 985.
(8) Lengsfield, B. H.; Saxe, P.; Yarkony, D. R. *J. Chem. Phys.* **1984**, *81*, 4549.
(9) Saxe, P.; Lengsfield, B. H.; Yarkony, D. R. *Chem. Phys. Lett.* **1985**, *113*, 159.
(10) Lengsfield, B. H.; Yarkony, D. R. Nonadiabatic Interactions Between Potential Energy Surfaces: Theory and Applications. In *State-Selected and State to State Ion-Molecule Reaction Dynamics: Part 2 Theory*; Baer, M., Ng, C.-Y., Eds.; John Wiley and Sons: New York, 1992; Vol. 82.
(11) Mead, C. A. *J. Chem. Phys.* **1983**, *78*, 807.
(12) Farantos, S. C.; Murrel, J. N.; Carter, S. *Chem. Phys. Lett.* **1984**, *108*, 367.
(13) Farantos, S. C. *Mol. Phys.* **1985**, *54*, 835.
(14) Perry, J. K.; Yarkony, D. R. *J. Chem. Phys.* **1988**, *89*, 4945.
(15) Pernot, P.; Grimes, R. M.; Lester, W. A., Jr.; Cerjan, C. *Chem. Phys. Lett.* **1989**, *163*, 297.
(16) Manaa, M. R.; Yarkony, D. R. *J. Chem. Phys.* **1990**, *93*, 4473.
(17) Atkins, D.; Fink, E. H.; Moore, C. B. *J. Chem. Phys.* **1970**, *52*, 1604.
(18) Fink, E. H.; Atkins, D. L.; Moore, C. B. *J. Chem. Phys.* **1972**, *56*, 900.
(19) Pibel, C. D.; Carlton, K. L.; Moore, C. B. *J. Chem. Phys.* **1990**, *93*, 323.
(20) Shavitt, I. The Method of Configuration Interaction. In *Modern Theoretical Chemistry*; Schaefer, H. F., Ed.; Plenum Press: New York, 1976; Vol. 3, pp 189.
(21) Yarkony, D. R. Electronic Structure Aspects of Nonadiabatic Processes in Polyatomic Systems. In *Modern Electronic Structure Theory*; Yarkony, D. R., Ed.; World Scientific: Singapore, 1995.
(22) Mead, C. A. *Chem. Phys.* **1980**, *49*, 23.
(23) Barclay, V. J.; Dateo, C. E.; Hamilton, I. P.; Kendrick, B.; Pack, R. T. *J. Chem. Phys.* **1995**, *103*, 3864.
(24) Kendrick, B.; Pack, R. T. *J. Chem. Phys.* **1996**, *104*, 7502.
(25) Kendrick, B.; Pack, R. T. *J. Chem. Phys.* **1996**, *104*, 7475.
(26) Schiff, L. I. *Quantum Mechanics*; McGraw Hill: New York, 1960.
(27) Zwanziger, J. W.; Grant, E. R. *J. Chem. Phys.* **1987**, *87*, 2954.
(28) Mead, C. A.; Truhlar, D. G. *J. Chem. Phys.* **1982**, *77*, 6090.
(29) Yarkony, D. R. *J. Chem. Phys.* **1996**, *105*, 10456−10461.
(30) Silverstone, H. J.; Sinanoglu, O. *J. Chem. Phys.* **1966**, *44*, 1899−1907.
(31) Huber, K. P.; Herzberg, G. *Molecular Spectra and Molecular Structure IV. Constants of Diatomic Molecules*; Van Nostrand Reinhold: New York, 1979.
(32) Yarkony, D. R. *J. Phys. Chem.* **1996**, *100*, 18612−18628.